Potential-Step Chronofluorometry of the Kinetics of Eosin Y Dianion Transfer across the 1,2-Dichloroethane/Water Interface

Takashi Kakiuchi* and Yoko Takasu†

Department of Physical Chemistry, Yokohama National University, Yokohama 240, Japan

Received: October 3, 1996; In Final Form: February 2, 1997[⊗]

Potential-step chronofluorometry, a new approach based on the measurement of the change in fluorescence intensity accompanied by interfacial ion transfer, has been applied to the study of the kinetics of Eosin Y dianions (EY^{2-}) transfer across the 1,2-dichloroethane (DCE)/water (W) interface. The standard rate constant is found to be 9.5×10^{-3} cm s^{-1} at 24 °C. This is an order of magnitude smaller than the value predicted by the Stokes' law and its diffusion coefficient in water, indicating the presence of greater friction against ion transfer at the interface. The dependence of the logarithm of the rate constant on the applied potential has a convex curvature, which does not conform to the Butler−Volmer current−potential characteristic with a potential-independent transfer coefficient. The observed curvature and the fact that the apparent transfer coefficient at the formal potential is 0.5 are instead well explained by the Goldman-type current−potential characteristic, which is based on the Nernst−Planck equation with the Goldman-type approximation, i.e., linear variation of electrochemical potential across the interfacial layer. The rate-determining step of the EY^{2-} ion transfer across the DCE/W interface can therefore be understood phenomenologically as an activationless process, as is the ion transport in homogeneous solution phase. The inadequacy of the Frumkin-type double-layer correction to the kinetics of charge transfer is suggested.

Introduction

Ion transfer across a liquid−liquid interface is a heterogeneous process taking place in an anisotropic medium at the interface where the density, viscosity, and molecular orientation of solvents are different from those in the adjacent bulk homogeneous phases.[1,2] This charge transfer in the heterogeneous environment is interesting, particularly in view of the dynamics of ion−solvent interactions.[3,4] Moreover, the interfacial ion transfer process has practical significance in various interfacial phenomena, including solvent extraction, micellar catalysis, phase transfer catalysis, and selective recognition of ions at ion-selective electrodes.[5,6] Recent molecular dynamics simulations of ion and electron transfers across the liquid−liquid interface have revealed microscopic aspects of this process, e.g., the role of a solvent finger to facilitate ion transfer, and helps us to envision movements of solvent molecules as well as an ion on a time scale of picoseconds.[3,7]

On the other hand, the rate of ion transfer has been studied experimentally using electrochemical techniques at polarized liquid−liquid interfaces from a macroscopic point of view.[1,8] Most experimental data so far obtained are for tetraalkylammonium ions and several monovalent anions. The transfer of all these ions is electrochemically a fast process; the apparent standard rate constants, k_0, for tetraalkylammonium ions across the nitrobenzene (NB)/water (W) interface are on the order of 0.1 cm s^{-1}.[9,10] From the transfer of a series of tetraalkylammonium ions, it has been suggested that the interfacial rate process is well described by a Goldman-type current potential characteristic and that the dielectric friction on the ion transfer is apparently enhanced at the interface.[11,12] However, these intriguing features of interfacial processes need to be further clarified, because most of the k_s values so far obtained are all close to the upper limit accessible to conventional electrochemical techniques. Recent measurements using a micro liquid−liquid interface suggested that the k_0 values for tetraalkylammonium ions could be even greater than 0.1 cm s^{-1}.[13,14]

A high double-layer capacitance and a large solution resistance inherent to the liquid−liquid interface are the two main sources imposing an upper bound to the measurable rate of charge transfer using conventional electrochemical techniques, such as the galvanostatic pulse method[15] and ac impedance method.[16] Voltage-controlled fluorometry[17−19] is less vulnerable to these two factors and is promising to obtain more reliable kinetic parameters for fluorescent ion transfer across the liquid−liquid interface.

In the present paper, we report the kinetics of Eosin Y dianion (EY^{2-}) transfer across the 1,2-dichloroethane (DCE)/W interface studied by using potential-step chronofluorometry (PSCF).[18,20] The change in the fluorescent intensity in the organic phase is monitored as a function of time after stepping the potential drop across the interface from a value without the fluorescent ion transfer to a value with the ion transfer. When the concentration of fluorescent ion is lower than tens of micromolar level and the time after the onset of ion transfer is short enough, the fluorescence intensity from the organic phase is proportional to the total charge transferred into the organic phase.[18] Under this condition, PSCF is equivalent to chronocoulometry for studying electrode reactions. The kinetic parameters of ion transfer can then be obtained from PSCF using theoretical treatments developed for chronocoulometry.[21]

Experimental Section

Materials. All chemicals used were of reagent grade. Span 80 was added to the DCE phase to suppress the convective motion of the solutions in the vicinity of the interface.

Methods. The cell is represented as

				1 μ M EY^{2-}		
		5 mM TPnACl	0.02 M TPnATPB	a M LiCl		
Ag	AgCl	0.01 M $MgCl_2$	0.5 mM Span 80	0.01 M Phosphate-Borate buffer(pH 8)	AgCl	Ag
		(**W**)	(**DCE**)	(**W**)		

where TPnACl and TPnATPB stand for tetrapentylammonium

* Corresponding author.

† Present address: National Institute of Sericulture and Entomological Science, Owashi 1-2, Tsukuba-shi, Ibaraki 305, Japan.

[⊗] Abstract published in *Advance ACS Abstracts,* July 1, 1997.

S1089-5647(96)03045-3 CCC: $14.00

chloride and tetrapentylammonium tetraphenylborate. Phosphate−borate was added to the aqueous phase for maintaining pH at 8.0, so that EY was in a dianionic form. The applied potential referred to the left-hand side of the cell is denoted as E. The configuration of the cell for PSCF measurements has been described elsewhere.[17] The polarized DCE/W interface formed at the orifice of a glass tube was adjusted to have a flat surface. The geometrical area of the interface was 0.166 cm^2. The methods for fluorescence and electrochemical measurements have been described elsewhere.[18] The laser beam of 0.65 mm diameter from a 15 mW Ar+ laser at 488 nm was reflected twice with mirrors and was led to the cell to shine on the interface from the DCE side of the interface. The angle of incidence was adjusted to about 75°. Time-dependent fluorescence when the potential was stepped from an initial potential, E_i, to a certain potential, E_f, sufficiently positive to cause the transfer of EY^{2-} from W to DCE was monitored usually at 500 μs intervals at the maximum emission of EY, 547 nm, in the DCE phase. After 200 ms, the potential was stepped back to E_i. The measurement at a given potential was repeated usually five times, and the signals were averaged for later data analysis. The time interval between the consecutive PSCF measurements was at least 10 s after the potential was stepped back to E_i to ensure the recovery of the concentration profile in the vicinity of the interface.

The solution resistance was compensated for by a positive feedback method using a positive feed-back circuit equipped in a laboratory-made two-electrode system composed of two operational amplifiers.[10] The degree of positive feedback is crucial to avoid the effect of solution resistance. Although the PSCF itself does not pick up the charging current, the indicial response of the interfacial potential to an applied potential step is affected by the time constant of the entire system. If we assume that the operational amplifiers used in the present system behave ideally, the ratio of the potential drop across the cell, e_{cell}, to the input potential, e_{in}, is expressed as

$$e_{cell}/e_{in} = -K/(1 + \tau s) \quad (1)$$

where $s = j\omega$. The amplitude, K, and the time constant, τ, are related to the parameters of the electrochemical cell through $K = (R_s/R_{ct})(1 - \xi) + 1$ and $\tau = R_s C_{dl}(1 - \xi)/K$, where R_s is the solution resistance, R_{ct} is the charge transfer resistance, C_{dl} is the double-layer capacitance, and ξ is the degree of iR compensation, which in the present approximation is unity when iR is fully compensated. The time constant is thus a function of ξ as well as other electrochemical parameters. We theoretically calculated fluorescent transients after a potential step was applied to the potentiostat at several values of ξ with varying the value of the standard rate constant of fluorescent ion transfer, k_0, using a method similar to that described elsewhere.[20] When the k_0 value is 10^{-3} cm s^{-1}, PSCF gives an accurate value of k_0 when $\xi > 0.95$. If the k_0 value is 2 orders of magnitude greater, ξ should be greater than 0.999, which was the typical degree of iR compensation in the present study.

All measurements were made at 24 ± 2 °C.

Results and Discussion

Figure 1 shows fluorescent transients after the potential was stepped from $E_i = 300$ mV to $E_i = 110$, 80, 70, and 50 mV at $a = 0.08$. The background signal in the absence of ion transfer, which was mainly due to stray light and fluorescent substances contaminated in the DCE phase, was subtracted from each signal for further analysis. Similar transients were recorded at the interval 10−20 mV between 130 and −30 mV.

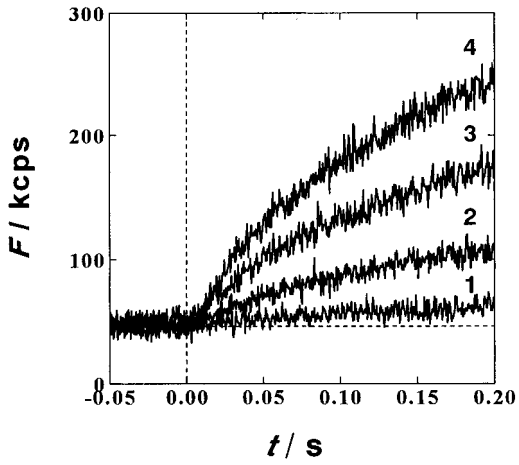

Figure 1. Potential-step transients of fluorescence for EY^{2-} transfer from W to DCE when the potential was stepped from 300 mV to 110 (1), 80 (2), 70 (3), and 50 (4) at 24.4 °C. The W phase contains 1 μ mol dm^{-3} EY^{2-}, 0.08 mol dm^{-3} LiCl, and 0.01 mol dm^{-3} phosphate buffer at pH 8.

Previously, we showed that the total fluorescent intensity from the DCE phase, $F^O(t)$, is related to electrochemical parameters of ion transfer through[18]

$$F^O(t) \propto \frac{\vec{k}\,{}^b c_i^W}{\lambda_2}\left[\exp(\lambda^2 t)\,\mathrm{erfc}(\lambda\, t^{1/2}) + \frac{2\lambda t^{1/2}}{\pi^{1/2}} - 1\right] \quad (2)$$

where $\lambda = \vec{k}/\sqrt{D^W} + \overleftarrow{k}/\sqrt{D^O}$, $\vec{k}$ and $\overleftarrow{k}$ and being the rate constant of ion transfer from the aqueous phase (W) to the DCE phase (O) and O to W, respectively, and D^W and D^O are the diffusion coefficient of the fluorescent ion in W and O.

Underlying assumptions in this equation are somewhat unrealistic; the angle of incidence of the excitation light was normal to the interface and the reflection of the incident light at the interface was negligible. In fact, even allowing for a finite angle of incidence, the reflection of the incident light at the interface, and the finite size of the beam diameter of the excitation light, we can still use eq 2, provided that the total amount of fluorescent ions in O is sufficiently small (see the Appendix). When $\lambda t^{1/2} > 5$, eq 2 is reduced to

$$F^O(t) \propto \vec{k}\,{}^b c_i^W\left[\frac{2t^{1/2}}{\lambda\pi^{1/2}} - \frac{1}{\lambda^2}\right] \quad (3)$$

The plot of $F^O(t)$ vs $\sqrt{t}$ should be a straight line, and we can estimate λ from the intercept of the plot at $F^O(t) = 0$.

Figure 2 shows $F^O(t)$ vs $\sqrt{t}$ curves replotted from the data in Figure 1. The solid lines are the least-squares fitting of the date at $t \geq 0.02$ s to straight lines, illustrating the linear relationship predicted by eq 3. Similar good linear relationships were observed at all other potentials studied. The intercept of the $\sqrt{t}$ axis, $\sqrt{t_1}$, was estimated from the least-squares fitting of the experimental points, taking account of the propagation of error. The values for $\sqrt{t_1}$ are plotted in Figure 3 as a function of the applied potential. The error bars indicate the 99% confidence interval estimated from triplicate measurements for each point.

The Butler−Volmer current−potential characteristic for a heterogeneous charge transfer process has the form

$$\frac{j}{zF} = k_0\left\{\exp\left[\alpha\frac{zF}{RT}(E - E^{0\prime})\right]c_0^W - \exp\left[-(1-\alpha)\frac{zF}{RT}(E - E^{0\prime})\right]c_0^O\right\} \quad (4)$$

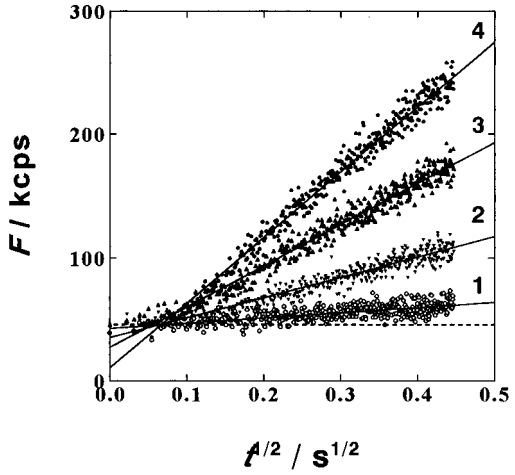

Figure 2. Change in fluorescence as a function of $\sqrt{t}$ replotted from data in Figure 1. Solid lines represent least-squares fittings of a straight line to experimental points.

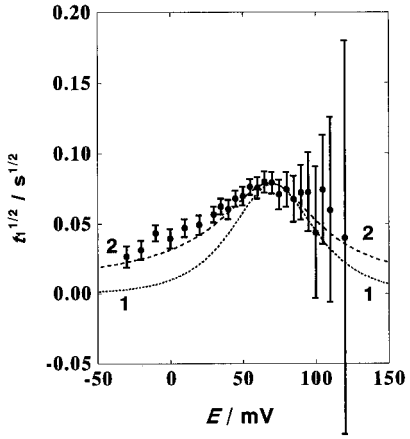

Figure 3. Variation of $\sqrt{t_1}$ with applied potential. Vertical bars indicate the 99% confidence interval. Curves 1 and 2 are calculated from eq 2 assuming that $\alpha = 0.5$ and from eq 4, respectively.

where j is the current density, k_0 is the apparent standard rate constant of ion transfer, z is the charge of the ion carrying current across the interface, F is the Faraday constant, α is the transfer coefficient, R is the gas constant, T is the temperature, $E^{0\prime}$ is the formal potential, and c_0^{W} and c_0^{O} are the surface concentrations of the ion in the aqueous side and the oil side of the interface. Curve 1 in Figure 3 is a theoretical curve calculated using eq 4, assuming that the transfer coefficient is 0.5 and is independent of the applied potential.

Curve 2 in Figure 3 is a theoretical prediction of the Goldman-type current−potential characteristic, which is based on the Nernst−Planck equation[22] and the Goldman-type assumption,[11] i.e., the linear variation of the electrochemical potential across the interface, instead of the linear variation of electrical potential, as is Goldman's original assumption:[23]

$$\frac{j}{zF} = k_0 \frac{y}{\sinh y}\{e^{y}c_0^{\mathrm{W}} - e^{-y}c_0^{\mathrm{O}}\} \qquad (5)$$

where $y = (zF/2RT)(E - E^{0\prime})$. Both curves 1 and 2 were superimposed on experimental points so that the peaks of the curves agreed with experimental points around the half-wave potential, 68 mV. In the potential range where $E > E_{1/2}$, large confidence intervals preclude the distinction between the two theoretical curves. However, in the potential range more negative than $E_{1/2}$, the experimental points are well represented by curve 2 in the entire range, while the Butler−Volmer model

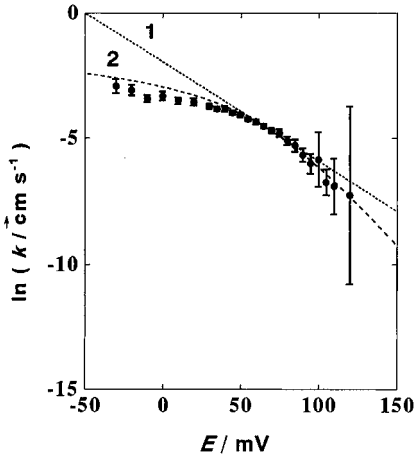

Figure 4. Change in ln k_0 with applied potential replotted from data in Figure 3. Vertical bars indicate the 99% confidence interval. Curves 1 and 2 are calculated from eq 2 assuming that $\alpha = 0.5$ and from eq 4, respectively.

underestimate $\sqrt{t_1}$ values. Thus the Goldman-type model well describes the dependence of the kinetic parameter of ion transfer on applied potential. The values of $\vec{k}$ were calculated from experimental $\sqrt{t_1}$ values using the microscopic reversibility assumption for the ion transfer, $\vec{k}/\overleftarrow{k} = \exp(zF/RT)(E - E^{0\prime})$, and the values of diffusion coefficients, $D^{\mathrm{W}} = 2.1 \times 10^{-6}$ cm s^{-1} and $D^{\mathrm{O}} = 2.8 \times 10^{-6}$ cm s^{-1}, estimated from cyclic voltammetry. The results are plotted in Figure 4 in the form of a Tafel plot. The experimental curve is not a straight line, showing a convex curvature, which is well described by the Goldman-type model, curve 2. It is notable that the slope of the plot at $E^{0\prime}$, 56 mV, is 1/2, as predicted by the Goldman-type model.

The value of k_0, 9.5×10^{-3} cm s^{-1}, is at least 1 order of magnitude smaller than k_0 values for the transfer of tetraethyl- and tetramethylammonium ions across the NB/W interface[9,10,13] and the DCE/W[14] whereas the diffusion coefficient of EY^{2-} is one-fifth of that of tetraethylammonium ion in the aqueous phase. The decrease in the rate of ion transfer across the interface is twice greater than what we can expect from the Stokes' law. Apparently, there is a certain factor that reduces, to a greater extent, the rate of EY^{2-} transfer across the interface in comparison with that of tetraalkylammonium ions. Recent molecular dynamics calculations for the transfer of small ions and molecules have found an activation barrier at the interface.[3,7,24] However, even in the transfer of small Cl^--like ions, the barrier height is about 20 kJ[7] and its magnitude seems to be very much dependent on the details of the models.

The observed k_0 value may be interpreted as the speed of an ion crossing the transition region, or the inner layer of the double layer, at the interface, whose thickness is believed to be on the order of 1 nm on average taken over a long time scale.[25] The observed value of k_0, 9.5×10^{-3} cm s^{-1}, means that an EY^{2-} ion needs 10 μs to cross the inner layer, which is much longer than the time scale of contemporary molecular dynamics calculation of liquid−liquid systems. For such a slow process, a phenomenological approach to the motion of particles in a viscous medium, e.g., the Nernst−Planck equation,[22] would be appropriate for the description of the process.[11,26] The success of the Goldman-type current−potential characteristic in the present case suggests the absence of an activation barrier at the interface, which parallels the situation of ion transport in a bulk homogeneous phase.

Another interesting aspect of the kinetics of EY^{2-} transfer across the interface is the magnitude of k_0, 9.5×10^{-3} cm s^{-1},

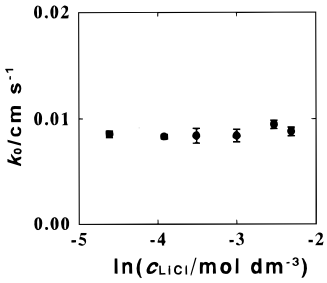

Figure 5. Dependence of k_0 on LiCl concentration in W. Vertical bars indicate standard deviation.

in comparison with its diffusion coefficient in the bulk homogeneous phase. In the Goldman-type model, k_0 is related to the diffusion coefficient of the transferring ion in the inner layer, D^σ, through

$$k_0 = D^\sigma/\Delta x \tag{6}$$

where Δx is the effective thickness of the inner layer. If we assume 1 nm for the thickness of the inner layer, the value of D^σ is 9.5×10^{-9} cm^2 s^{-1}, which is only two hundredths of the diffusion coefficient of EY^{2-} in the bulk aqueous phase. Similar significant deceleration has been observed for the transfer of tetraalkylammonium ions across the NB/W interface, and the enhancement of dielectric friction at the interface has been proposed as a possible mechanism.[11] EY^{2-} has one localized negative charge at the carboxylate group, which can be responsible for the dielectric friction. The other negative charge is delocalized in the xanthene ring. Another possible factor that slows the ion transfer at the interface is the temporary adsorption of EY^{2-}, because the presence of a localized charge in a large lipophilic xanthene molecule probably endows EY^{2-} ions with surface activity. The adsorption is, if any, weak, however, as no conspicuous postwave or prewave[27] has been detected on cyclic voltammograms of EY^{2-} transfer.

The applicability and appropriateness of the double-layer effect on ion transfer across the electrified interface have been discussed both theoretically and experimentally.[9,16,28−35] If a Frumkin-type double-layer effect[36] on the kinetics of charge transfer is existent, the change in the concentration of supporting electrolytes should affect the observed kinetic parameters. However, no such dependence of the parameters has been observed for picrate ion transfer[16] and other monovalent ion transfers across the interface.[33] Since the latter two studies employed an ac impedance method for kinetics measurements, it would be worthwhile to see the dependence of kinetic parameters on the concentration of supporting electrolytes in the present system, which differs from the previous studies in both experimental techniques and the type of ion.

We measured k_0 values at four other concentrations of LiCl in W, 0.1, 0.2, 0.3, 0.4, and 1.0 mol dm^{-3}. The results are plotted in Figure 5. Each point represents the average value of triplicate measurements, and the magnitude of standard deviation is indicated as a vertical bar at each point. Obviously, there is no significant change in k_0 with the LiCl concentration, whereas a theoretical calculation based on the Gouy−Chapman theory and the electrocapillary data predicts at least a 20% decrease in k_0 when the LiCl concentration is varied from 0.01 to 0.1 mol dm^{-3}.[33] The observed insensitiveness of k_0 on the supporting electrolyte concentration (Figure 5) is consistent with the previous results for the transfer of monovalent ions across the NB/W interface.[16,33] It is therefore likely that the Frumkin-type double-layer correction is not appropriate for extracting "true" values of kinetic parameters. There are two conceivable reasons for the apparent absence of the double-layer effect. First is the oversimplification of the double-layer structure inherent to the Gouy−Chapman theory,[37,38] and second is the concept of the Frumkin-type correction itself. Despite the simplification implied in the Gouy−Chapman or Poisson−Boltzmann equation,[39] the Gouy−Chapman model gives a reasonable picture for the diffuse part of the electrical double layer at the liquid−liquid interface in the case of 1:1 electrolytes,[40−42] suggesting that the problem lies in the Frumkin correction.

Under the regime of a linear irreversible process which leads to the Nernst−Planck equation, the flow is proportional to the gradient of electrochemical potential.[43] If a reaction plane is located within the electrical double layer, the electrical potential of the reaction plane is generally different from the potential in the bulk phase, which the idea of the Frumkin correction stems from. Usually, the Frumkin correction calculates the concentration of reactants at the reaction plane, assuming the Boltzmann distribution of ionic reactants. This model premises that the distribution of ionic reactants in response to the potential distribution in the vicinity of the interface is in thermodynamic equilibrium. In other words, the electrochemical potential of the reactant is uniform throughout the diffuse part of the double layer; the change in the electric potential is exactly compensated by the change in the concentration of the reactant. Then, there exits no energetic driving force across the diffuse layer of the double layer for ion transport. While the relaxation time of the electrical double layer is presumably very fast, i.e., on the order of picoseconds,[44] the rate of charge transfer across the interface is much slower as described above. The establishment of thermodynamic equilibrium in ion distribution thus seems to be a sound assumption. It is therefore concluded that the legitimacy of a Frumkin-type double-layer correction on kinetic parameters of charge transfer across the interface is dubious, while other types of double-layer effects on heterogeneous charge transfer processes, e.g., the effect of enhanced ion−ion correlation in the double layer on charge transfer, cannot be ruled out.

Conclusion

The apparent standard rate constant of EY^{2-}, 9.5×10^{-3} cm s^{-1}, is lower than the upper bound experimentally accessible using the present technique, PSCF, providing more unequivocal evidence for the presence of slower ion transfer across the interface in comparison with the ion transport in the bulk solution phase. The rate of EY^{2-} ion transfer across the DCE/W interface is also slower than what is expected from the similar deceleration of ion transfer across the interface for symmetrical tetraethylammonium ions even after taking account of the difference in the hydrodynamic radius of the two ions. The weak adsorption of EY^{2-} ions at the interface is suggested to be a probable factor for the apparent slower transfer. Macroscopically, the process can be explained without assuming the presence of an activation barrier at the interface against the ion transfer. The apparent absence of the double-layer effect of the Frumkin-type on the EY^{2-} transfer is indicative of the necessity of reviewing the classical Frumkin-type double-layer correction.

Acknowledgment. This work was supported in part by Grants-in-Aid 05640568 and 08640769 for Scientific Research from the Ministry of Education, Science and Culture, Japan.

Appendix

We consider the transfer of a fluorescent ion from W to O. The excitation light is introduced from the O phase to the W

phase with the angle of incidence, θ, satisfying the condition of total reflection, where the O phase is assumed to have a larger refractive index than the W phase. Fluorescence in W due to the evanescent wave of the excitation light is assumed to be negligible. We assume that fluorescent ions in O are excited by both incident light and reflected light, independently, and there is no concentration quenching of the fluorescence.

a. Fluorescence Due to Incident Light. The Lambert−Beer's law in this case is represented by

$$dI^{O}(x,t) = I^{O}(x,t)c^{O}(x,t)\kappa^{O} \sec\theta\, dx \quad (7)$$

where $I^{O}(x,t)$ is the intensity of light, $c^{O}(x,t)$ is the concentration of the fluorescent ion in O, κ is the absorption coefficient of the fluorescent ion, x is the distance normal to the interface, and t is time. The direction of the x axis is pointing toward the O phase, and its origin is taken at the interface. The incident light comes from the infinity in O, where $c^{O}(x,t) = 0$. The intensity of the incident light is then

$$I^{O}(x,t) = I_0 \exp[\kappa^{O} \sec\theta \int_{\infty}^{x} c^{O}(\zeta,t)\, d\zeta] \quad (8)$$

On the other hand, the fluorescence from a volume element of thickness dx with unit area is given by

$$dF(x,t) = \kappa^{O}\Phi^{O}I^{O}(x,t)\, c^{O}(x,t)\, dx \quad (9)$$

We assume that the area of the interface is much larger than the area illuminated by the excitation light. When the incident light is a cylindrical light beam having a uniform radius, r, the fluorescence intensity from the fluorescent ion within the beam path is expressed as

$$F_1(t) = \kappa^{O}\Phi^{O}\pi r^2 \sec\theta \int_{0}^{\infty} I^{O}(x,t)\, c^{O}(x,t)\, dx \quad (10)$$

b. Fluorescence Due to Reflected Light. The intensity of light reached at the interface is

$$I^{O}(0,t) = I_0 \exp[\kappa^{O} \sec\theta \int_{\infty}^{0} c^{O}(\zeta,t)\, d\zeta] \quad (11)$$

and the Lambertn-Beer's law for the reflected light is

$$dI^{O}(x,t) = -I^{O}(x,t)c^{O}(x,t)\kappa^{O} \sec\theta\, dx \quad (12)$$

The intensity of the reflected light is then given by

$$I^{O}(x,t) = kI^{O}(0,t) \exp[k^{O} \sec\theta \int_{0}^{x} c^{O}(\zeta,t)\, d\zeta] \quad (13)$$

where k is the reflectance of the light at the interface. From eqs 3 and 8, the fluorescence from the beam path of the reflected light is

$$F_2(t) = \kappa^{O}\Phi^{O}\pi\, r^2 \sec\theta\, kI^{O}(0,t) \int_{0}^{\infty} I^{O}(x,t)\, c^{O}(x,t)\, dx \quad (14)$$

The total fluorescence intensity in the O phase is $F_T(t) = F_1 + F_2$.

c. Relationship with Mass Transport across the Interface. Substituting an appropriate expression for $c^{O}(x,t)$ in eqs 10 and 14 by solving the problem of mass transfer of the fluorescent ion, we obtain the fluorescence intensity as a function of time and of the concentration of the fluorescent ion in the W phase, c^{W}.

Of practical importance is the case when all the arguments of the exponential terms on the rhs of eqs 10 and 14 are negligible. This condition is fulfilled when either c^{W} or t is small.[20] F_T is then given by

$$F_T(t) = \kappa^{O}\Phi^{O}\pi\, r^2 \sec\theta\, I_0(1+k) \int_{0}^{\infty} c^{O}(x,t)\, dx \quad (15)$$

On the other hand, the total amount of fluorescent ions in DCE at a given time is equal to the charge transferred into the DCE phase when $c^{O}(x,t{=}0) = 0$, as is the case of usual electrochemical measurements:

$$\int_{0}^{\infty} c_i^{O}(x,t)\, dx = \frac{1}{z_i FA} \int_{0}^{t} i(t)\, dt \quad (16)$$

where $i(t)$ is the current across the interface carried by the fluorescent ion, z_i is the charge on the ion in the signed unit, F is the Faraday constant, and A is the area of the interface. From eqs 15 and 16, we obtain

$$F^{O}(t) = \frac{\kappa^{O}\Phi^{O}I_0\pi r^2 \sec\theta}{z_i FA}(1+k) \int_{0}^{t} i(t)\, dt \quad (17)$$

The proportionality between the fluorescence intensity and the total charge of transferred ions shown in the previous model[18] thus holds also in the present case: the nonzero angle of incidence, the nonzero reflectance of the incident light, and a finite size of the beamed area of the interface.

References and Notes

(1) Samec, Z.; Kakiuchi, T. In *Advances in Electrochemistry and Electrochemical Science*; Gerischer, H., Tobias, C. W., Eds.; VCH: Weinheim, 1995; p 297.
(2) Benjamin, I. *Chem. Rev.* **1996**, *96*, 1449.
(3) Schweighofer, K. J.; Benjamin, I. *J. Phys. Chem.* **1995**, *99*, 9974.
(4) Benjamin, I. *Acc. Chem. Res.* **1995**, *28*, 233.
(5) Senda, M.; Kakiuchi, T.; Osakai, T. *Electrochim Acta* **1991**, *36*, 253.
(6) Volkov, A. G.; Deamer, D. W. In *Liquid-Liquid Interfaces: Theory and Methods*; CRC Press: Boca Raton, 1996.
(7) Benjamin, I. *Science* **1993**, *261*, 1558.
(8) Samec, Z. In *Liquid-Liquid Interfaces: Theory and Methods*; Volkov, A. G., Deamer, D. W., Eds.; CRC Press: Boca Raton, 1996; p 155.
(9) Wandlowski, T.; Marecek, V.; Holub, K.; Samec, Z. *J. Phys. Chem.* **1989**, *93*, 8204.
(10) Kakiuchi, T.; Noguchi, J.; Kotani, M.; Senda, M. *J. Electroanal. Chem. Interfacial Electrochem.* **1990**, *296*, 517.
(11) Kakiuchi, T. *J. Electroanal. Chem. Interfacial Electrochem.* **1992**, *322*, 55.
(12) Kakiuchi, T.; Noguchi, J.; Senda, M. *J. Electroanal. Chem. Interfacial Electrochem.* **1992**, *327*, 63.
(13) Marecek, V.; Lhotsky, A.; Račinský, S. *Electrochim. Acta* **1995**, *40*, 2905.
(14) Beattie, P. D.; Delay, A.; Girault, H. H. *Electrochim. Acta* **1995**, *40*, 2961.
(15) Samec, Z.; Mareček, V.; Homolka, D. *Faraday Dicuss. Chem. Soc.* **1984**, *77*, 197.
(16) Osakai, T.; Kakutani, T.; Senda, M. *Bull. Chem. Soc. Jpn.* **1985**, *58*, 2626.
(17) Kakiuchi, T.; Takasu, Y.; Senda, M. *Anal. Chem.* **1992**, *64*, 3096.
(18) Kakiuchi, T.; Takasu, Y. *Anal. Chem.* **1994**, *66*, 1853.
(19) Ding, Z.; Wellington, R. G.; Brever, P. F.; Girault, H. H. *J. Phys. Chem.* **1996**, *100*, 10658.
(20) Kakiuchi, T.; Takasu, Y. *J. Electroanal. Chem. Interfacial Electrochem.* **1995**, *381*, 5.
(21) Christie, J. H.; Lauer, G.; Osteryoung, R. A. *Anal. Chem.* **1963**, *35*, 1979.
(22) Nernst, W. *Z. Phys. Chem.* **1888**, *2*, 613.
(23) Goldman, D. E. *J. Gen. Physiol.* **1943**, *27*, 37.
(24) Hayoun, M.; Meyer, M.; Turq, P. *J. Phys. Chem.* **1994**, *98*, 6626.
(25) Benjamin, I. *J. Chem. Phys.* **1992**, *97*, 1432.
(26) Benjamin, I. *J. Chem. Phys.* **1992**, *96*, 577.
(27) Nicholson, R. S.; Shain, I. *Anal. Chem.* **1964**, *36*, 706.
(28) d'Epenoux, B.; Seta, P.; Amblard, G.; Gavach, C. *J. Electroanal. Chem. Interfacial Electrochem.* **1979**, *99*, 77.
(29) Samec, Z. *J. Electroanal. Chem.* **1979**, *99*, 197.
(30) Buck, R. P.; Bronner, W. E. *J. Electroanal. Chem. Interfacial Electrochem.* **1986**, *197*, 179.
(31) Shao, Y.; Campbell, J. A.; Girault, H. *J. Electroanal. Chem. Interfacial Electrochem.* **1991**, *300*, 415.

(32) Samec, Z.; Marecek, V. *J. Electroanal. Chem. Interfacial Electrochem.* **1992**, *333*, 319.

(33) Kakiuchi, T.; Noguchi, J.; Senda, M. *J. Electroanal. Chem. Interfacial Electrochem.* **1992**, *336*, 137.

(34) Samec, Z.; Kakiuchi, T.; Senda, M. *Electrochim. Acta* **1995**, *40*, 2971.

(35) Senda, M. *Electrochim. Acta* **1995**, *40*, 2993.

(36) Frumkin, A. N. *Z. Phys. Chem.* **1933**, *164*, 121.

(37) Gouy, G. *J. de Phys.* **1910**, *9* (4), 457.

(38) Chapman, D. L. *Phil. Mag.* **1913**, *25*, 475.

(39) McQuarrie, D. A. In *Statistical Mechanics*, Harper & Row: New York, 1976; Chapter 15.

(40) Gros, M.; Gromb, S.; Gavach, C. *J. Electroanal. Chem.* **1978**, *89*, 29.

(41) Kakiuchi, T.; Senda, M. *Bull. Chem. Soc. Jpn.* **1983**, *56*, 1753.

(42) Torrie, G. M.; Valleau, J. P. *J. Electroanal. Chem. Interfacial Electrochem.* **1986**, *206*, 69.

(43) Callen, H. B. *Thermodynamics*; John Wilery & Sons: New York, 1960; Chapter 15.

(44) Blum, L.; Huckaby, D. A.; Legault, M. *Electrochim. Acta* **1996**, *41*, 2207.